



















**Highlights on Cool Stars 22 Splinter Session;
Planet-Host Cool Dwarfs: Star-Planet Connection and Tracing Planetary Formation and Composition**

NEDA HEJAZI ¹, EMILIO MARFIL ^{2,3}, DAVID R. CORIA ¹, DIOGO SOUTO ⁴, ZACHARY G. MAAS ⁵,
ZHOUJIAN ZHANG ^{6,*}, KATIA CUNHA ⁷, YAKIV PAVLENKO ⁸, IAN J. M. CROSSFIELD ¹, NATALIE R. HINKEL ⁹,
VARDAN ADIBEKYAN ¹⁰, ULRIKE HEITER ¹¹, AISHWARYA IYER ^{12,13,†}, DAVID MONTES ², ADAM D. RAINS ¹¹,
HENRIQUE REGGIANI ¹⁴, ADAM WHEELER ¹⁵ AND SHUO ZHANG ¹⁶

¹Department of Physics and Astronomy, University of Kansas, Lawrence, KS 66045, USA

²Departamento de Física de la Tierra y Astrofísica and IPARCOS-UCM (Unidad de Física de Partículas y del Cosmos de la UCM),
Facultad de Ciencias Físicas, Universidad Complutense de Madrid, 28040 Madrid, Spain

³Hamburger Sternwarte, Universität Hamburg, Gojenbergsweg 112, 21029 Hamburg, Germany

⁴Departamento de Física, Universidade Federal de Sergipe, Av. Marcelo Deda Chagas, S/N Cep 49.107-230, São Cristóvão, SE, Brazil

⁵Department of Astronomy, Indiana University, Bloomington, IN 47405, USA

⁶Department of Astronomy and Astrophysics, University of California, Santa Cruz, CA 95064, USA

⁷Department of Astronomy and Steward Observatory, University of Arizona, Tucson, AZ 85721, USA

⁸Instituto de Astrofísica de Canarias, E-38205 La Laguna, Tenerife, Spain

⁹Department of Physics and Astronomy, Louisiana State University, Baton Rouge, LA 70803, USA

¹⁰Institute of Astrophysics and Space Sciences, 4150-762 Porto, Portugal

¹¹Department of Physics and Astronomy, Uppsala University, Box 516, SE-75120 Uppsala, Sweden

¹²NASA Goddard Space Flight Center, Greenbelt, MD 20771, USA

¹³Arizona State University, School of Earth and Space Exploration, 525 E. University Dr., Tempe AZ 85281

¹⁴NOIRLab, Gemini South, Cerro Pachón, Chile

¹⁵Department of Astronomy, Ohio State University, Columbus, OH 43210, USA

¹⁶Department of Astronomy, Tsinghua University, Beijing 100084, China.

ABSTRACT

We present a summary of our splinter session as part of Cool Stars 22 that was held in San Diego, on June 27, 2024. The session time was allocated to eight talks and seven short poster presentations about the physical parameters and elemental abundances of cool dwarfs as well as chemical links between these stars and their planets. Due to their complex spectra, the spectroscopic analyses of cool dwarfs have proven to be challenging. Accordingly, the major goal of the session was to present the most recent techniques for measuring the parameters and chemical composition of cool dwarfs using advanced observations. These measurements would be of critical importance in exploring star-planet connections and tracing the formation pathway of planetary systems.

1. INTRODUCTION

Owing to their small mass and radius, cool dwarfs ($T_{\text{eff}} < 4700$ K) are optimal and primary targets for transit and radial velocity studies of planets outside our solar system. There likely exists at least one planet orbiting around each cool dwarf (e.g. Dressing & Charbonneau 2013, 2015; Tuomi et al. 2014; Hardegree-Ullman et al. 2019), and given their ubiquity in the Galaxy, these stars dominate the general incidence rates of planets around main-sequence stars. Moreover, because of the tendency of cool dwarfs to host exoplanets that are the targets of atmospheric characterization studies, these stars themselves are main candidates for complementary chemical measurements.

A planet and its host star are believed to originate from the same collapsing molecular cloud, and there is a chemical correlation between these two components. The comparison between the chemical abundances of planets and their host stars could then help to elucidate the formation mechanism and chemical evolution of planetary systems. To this end, the chemical abundances of both planets and

* NASA Sagan Fellow

† NASA Postdoctoral Program Fellow

their parent stars need to be measured with a decent accuracy. Considering the unprecedented near- and mid-infrared (NIR and MIR) sensitivity of James Webb Space Telescope (JWST), the atmospheric and/or surface composition of exoplanets are being measured with high accuracy. However, a large fraction of cool dwarfs with confirmed exoplanet(s) do not have uniformly measured chemical abundances, making direct comparisons with the JWST-derived planetary abundances impossible.

The spectra of these low-mass cool dwarfs are dominated by millions of molecular lines in the blue (AlH, MgH), optical (e.g., TiO and CaH) and near-infrared (NIR, e.g., H₂O) regions, which are blended with each other and many atomic lines. This causes a significant flux depression and, in turn, makes identifying the continuum level in many wavelength areas challenging. Combined with the substantial line crowding, established methodologies for FGK-type dwarfs and giant stars are therefore inappropriate for cooler dwarfs. This indicates the urgent need for characterizing the atmosphere and measuring the chemical abundances of cool dwarf stars. Despite the significant progress that has been made in determining the physical parameters of cool dwarfs using spectral synthesis (e.g. Rajpurohit et al. 2014; Lindgren et al. 2016; Lindgren & Heiter 2017; Rajpurohit et al. 2018; Passegger et al. 2018, 2019; López-Valdivia et al. 2019; Souto et al. 2017, 2020; Pavlenko et al. 2021; Souto et al. 2021; Zhang et al. 2021; Hejazi et al. 2022; Pavlenko et al. 2022; Souto et al. 2022; Marfil et al. 2021; Wanderley et al. 2023), the consistency in parameter values from different model atmospheres, wavelength ranges, and resolutions is still under debate (e.g. Passegger et al. 2022).

Moreover, measuring the individual elemental abundances of these cool dwarfs using line-by-line model fitting is still in the early stage (e.g. Souto et al. 2017; Abia et al. 2020; Shan et al. 2021; Souto et al. 2022; Hejazi et al. 2023; Hejazi et al. 2024; Melo et al. 2024; Tabernero et al. 2024). The accuracy of inferred elemental abundances highly depends on model atmospheres and atomic and molecular line lists used in spectral synthesis. Although remarkable progress has been made in modeling the atmospheres of cool dwarfs, there are still deficiencies in these models that can lead to significant inconsistencies between the observed and synthetic spectra in some wavelength ranges. Furthermore, while many atomic/molecular line lists have been updated in the last decade, the insufficiency of line data is also a major source of errors in synthesizing cool-dwarf spectra. One of the main goals of this splinter was to talk about the current methods and possible future improvements for measuring the physical parameters and individual elemental abundances of cool dwarfs with sufficiently high accuracy, and prospects for automating such techniques, which could be applied to large surveys.

Another major focus of our splinter was to discuss how the chemistry of cool planet-host stars can relate to the formation pathway, interior structure, and composition of exoplanets. For example, stellar abundances of volatile elements such as H, C, N, O, and S could provide fundamental insights into the formation mechanisms, evolution, and chemical composition of giant planets. (e.g. Fortney 2012; Brewer & Fischer 2016; Bedell et al. 2018; Delgado Mena et al. 2021; Turrini et al. 2021; Crossfield 2023). In particular, the comparison between the C/O abundance ratio of stars and their planets could give important clues on planet formation location relative to ice lines (e.g. Öberg et al. 2011). Isotopologue abundance ratios such as $^{12}\text{C}/^{13}\text{C}$, $^{14}\text{N}/^{15}\text{N}$, $^{16}\text{O}/^{18}\text{O}$ are also of importance to trace the planet formation and accretion histories (e.g. Zhang et al. 2017, 2021a,b; Barrado et al. 2023; Nomura et al. 2023; Bergin et al. 2024; Yoshida et al. 2024). The isotopologue ratio measurements of Jupiter-class exoplanets have been normally compared to the solar values rather than the corresponding values of their host stars, as the detection of minor isotopologues in cool dwarfs has presented difficulties. Nevertheless, it has been shown that these CNO isotopologue measurements are feasible in solar twin stars (Botelho et al. 2020; Coria et al. 2023, 2024) and down to cool M dwarf stars (Tsuji 2016; Crossfield 2019; Xuan et al. 2024).

The splinter session also aimed to discuss the characterization of rocky, terrestrial worlds. The chemical composition of rocky planets can be obtained by their measured mass and radius using interior models (e.g. Valencia et al. 2006; Seager et al. 2007). However, the interior models are highly degenerate (e.g. Rogers & Seager 2010), such that multiple interior models with different chemical compositions can be associated with the same mass and radius. One way to break the degeneracy is to utilize the elemental abundances of host stars to better constrain the composition of planets (e.g. Rogers & Seager 2010; Dorn et al. 2015; Brugger et al. 2017). Certain key elements may have an especially large effect on the bulk composition of rocky planets and/or their atmospheres, such as C, O, Mg, Si, and Fe (e.g. Bond et al. 2010; Brewer & Fischer 2016; Dorn et al. 2017). To a first-order approximation, the chemical abundances of refractory elements associated with a rocky planet are assumed to be identical to those of its host star (e.g. Hinkel & Unterborn 2018; Unterborn et al. 2018). If stellar values are representative of bulk planetary abundances, then the ratios of Mg/Fe and Si/Fe can be used to constrain planets’ relative core and mantle mass fractions by calculating the core chemistry and equilibrium mantle mineralogy (e.g. Unterborn et al. 2023).

In conclusion, the determination of physical parameters and chemical abundances of cool dwarfs are of paramount importance to advance our understanding of star-planet chemical connections. The investigation of numerous planetary systems around cool dwarfs could improve the previous findings and lead to much more robust relations between the properties of planets and their host stars. This was our main motivation to hold this splinter session and highlight the most recent studies of cool-dwarf characterization. In the following sections, we summarize the oral talks and then list each poster pop that were presented in our session. Some details of our session can be found in the website of the splinter session: <https://cs22-splinter-cool-dwarfs.webflow.io/>

2. LINKING THE PRIMORDIAL COMPOSITION OF STARS TO THE PRESENT-DAY COMPOSITION OF THEIR ROCKY EXOPLANETS

Vardan Adibekyan et al.

When modeling the interiors of rocky planets, a one-to-one correlation between the composition of the planet and that of its host star is typically assumed (e.g. Thiabaud et al. 2015; Dorn et al. 2015). However, this assumption has not yet been observationally confirmed. We analyzed a sample of 32 low-mass planets (with relative uncertainties in mass and radius better than 25% and 8%, respectively) orbiting 30 FGK-type stars to investigate the compositional link between stars and their planets. Compared to our previous study (Adibekyan et al. 2021), we determined the primordial compositions of the host stars and used a planetary interior model that also accounts for the presence of water (primarily in steam form).

We derived the primordial stellar abundances of C, O, Mg, Si, and Fe from their present-day atmospheric values, demonstrating that while individual elemental abundances can vary significantly over time, the ratios between them remain relatively stable over the main sequence for the cool dwarfs in our sample. We then used the primordial abundances as input for the stoichiometric model presented by Santos et al. (2015) to estimate the iron-to-silicate mass fraction ($f_{\text{iron,prim}}^{\text{star}}$) of the protoplanetary disks.

We employed a three-component planetary interior model (Dorn et al. 2015; Luo et al. 2024) to derive the compositions of the planets based on their mass and radius. We found a statistically significant correlation between the iron-to-silicate mass fraction of planets and their host stars. As also found in Adibekyan et al. (2021), the range of $f_{\text{iron}}^{\text{planet}}$ is significantly broader than that of their building blocks. This indicates that while the primordial composition of the protoplanetary disk sets a baseline for planetary composition, various processes during planet formation and evolution can

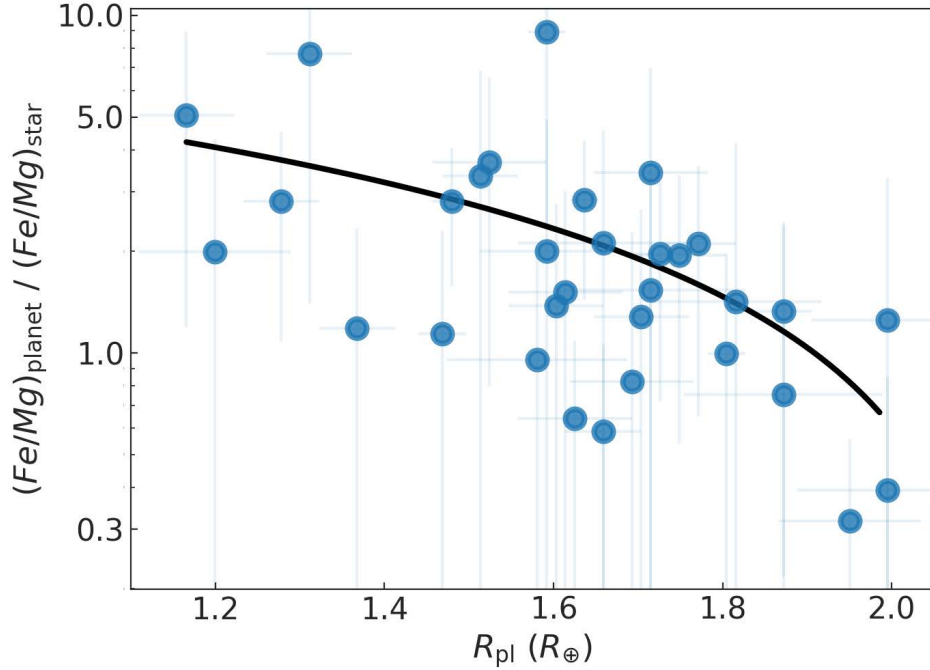


Figure 1. The Fe/Mg abundance ratio of planets and their host stars as a function of planetary radius. The black solid line represent the results of the Ordinary Least Squares regression (p-value ~ 0.006) performed on the linearly scaled data.

lead to substantial deviations in the iron-to-silicate mass fraction of the resulting planets compared to their original building materials. Additionally, we compared the Fe/Mg ratios in planets and their host stars (see Figure 1), finding a variation of 0.3 to 10 times between the two. This ratio was also found to correlate with planetary radius, further indicating that processes within the protoplanetary disk significantly influence the final composition of rocky planets.

In summary, we confirm previous results (Adibekyan et al. 2021) suggesting that while a correlation exists between the composition of rocky planets and their host stars, the assumption of a strict one-to-one elemental abundance relationship is not supported by our observations.

3. DETERMINING THE CHEMICAL COMPOSITION OF COOL DWARF STARS

Ulrike Heiter

We focus here on recent advances in the determination of the chemical composition of M dwarfs. Regarding metallicity determination, many works have been published, and a few examples can be seen in the other sections of this splinter summary. In the following we discuss determinations of individual element abundances for M dwarfs. These are still rare, but are becoming increasingly feasible with the availability of a number of high-resolution¹ near-infrared spectrographs at 2- to 10-m class telescopes².

Optical low- to medium-resolution spectra have also been used for this purpose. Maldonado et al. (2020) applied principal component analysis and sparse Bayesian methods to high-resolution spectra smoothed to low resolution and determined abundances of 15 elements for about 200 M dwarfs. Hejazi et al. (2022) applied a pipeline for deriving α -element abundances based on synthetic spectra

¹ Here, spectral resolution (resolving power) $R = \lambda/\Delta\lambda$ is regarded to be high for $R = 20\,000 \dots 100\,000$, while low/medium resolution corresponds to $R = 2000 \dots 7000$.

² NIRSPEC (Keck II), APOGEE (Apache Point Observatory), IGRINS (McDonald Observatory), CARMENES (Calar Alto), GIANO-B (Telescopio Nazionale Galileo), IRD (Subaru), HPF (Hobby-Eberly Telescope), SPIRou (CFHT), NIRPS (ESO 3.6m), CRIRES+ (VLT), SPIP (Télescope Bernard Lyot, start 2025)

fitting to low-resolution spectra of around 3700 M dwarfs. [Rains et al. \(2024\)](#) developed a data-driven machine learning method to determine Ti abundances (see Sect. 6).

Regarding abundances from high-resolution near-infrared spectra, pioneering works have been published by [Veyette et al. \(2017\)](#), [Abia et al. \(2020\)](#), [Ishikawa et al. \(2020\)](#), [Shan et al. \(2021\)](#), [Ishikawa et al. \(2022\)](#), and [Souto et al. \(2022\)](#). [Veyette et al. \(2017\)](#) developed an equivalent width method for the determination of Ti abundances from NIRSPEC spectra of around 40 stars, while [Abia et al. \(2020\)](#) and [Shan et al. \(2021\)](#) used CARMENES spectra to derive abundances for the neutron-capture elements Rb, Sr, Zr (~ 60 stars) and for vanadium (135 stars), respectively.

The other three works are presented in more detail in the following. [Ishikawa et al. \(2020\)](#) analysed 53 spectral lines of 8 elements in CARMENES Y- and J-band spectra ($R = 80\,000$, 0.96 to $1.3\,\mu\text{m}$) for a sample of six M dwarfs ($T_{\text{eff}} \gtrsim 3200\text{ K}$) in binaries with G/K stars. Abundances were derived from a comparison of observed and synthetic equivalent widths. The abundance precision was in general estimated to be ~ 0.2 dex, from combining several sources of uncertainty, while the precision for Ti was ~ 0.3 to 0.5 dex for the coolest stars. The abundances were found to agree with those of the primary stars within the estimated precision. Their Fig. 2 nicely shows the behaviour of the Na line at 1083.8 nm for different Na abundances spanning from -0.4 to $+0.4$ dex, and the good fit of synthetic and observed spectra for the derived abundances. This work also contains an investigation and summary of various sensitivity effects encountered in the analysis. A high sensitivity of abundances to surface gravity ($\log g$) was found, due to the large pressure broadening at high $\log g$. Furthermore, the sensitivity of the line strength to abundances of elements other than the absorber was found to be important for many lines, mainly due to the contribution of electron donors to electron pressure, which increases the continuous absorption by H^- . A demonstration for the case of an Fe line at different Na abundances can be found in their Fig. 6. Finally, it was pointed out that the strength of Ti lines is sensitive to the O abundance due to the formation of TiO .

[Ishikawa et al. \(2022\)](#) extended the analysis to cooler temperatures, analysing 71 spectral lines of 8 elements in Subaru/IRD Y- and J-band spectra ($R = 70\,000$) for a sample of 13 mid- to late M dwarfs (most of them with T_{eff} around 3100 K). Their Fig. 8 shows the observed line profiles of the Na line at 1083.8 nm for three different Na abundances between -0.3 to $+0.45$ dex. In this case, the abundance precision was in general estimated to be 0.2 to 0.4 dex, and for Ti up to 0.7 dex. They derived abundance ratios similar to solar values, for a metallicity range of about -0.6 to $+0.4$ dex. The main limitation for the abundance quality was found to be the uncertainty of the effective temperature. It was pointed out that the abundances for the late M dwarfs still need to be verified using visual binaries.

[Souto et al. \(2022\)](#) analysed 113 spectral lines of 12 elements (including two Na lines at 1637.4 and 1638.9 nm) in APOGEE H-band spectra ($R = 22\,500$, 1.5 to $1.7\,\mu\text{m}$) for a sample of 21 M dwarfs (half of them in binaries with FGK stars, the other half with interferometric angular diameters). Abundances were derived from a comparison of synthetic and observed spectra. The abundance uncertainties were estimated to be ~ 0.1 dex. In the case of the binaries, abundance differences between components ranged from 0 to 0.2 dex, in a few cases reaching 0.3 dex. Their Fig. 1 shows example spectra for the whole wavelength range for a metal-poor and a solar-metallicity star.

[Na/Fe] ratios of M dwarfs based on IRD spectra are compared to those of FGK stars (from [Adibekyan et al. 2012](#)) in Fig. 13 of [Ishikawa et al. \(2022\)](#), while [Na/Fe] ratios of M dwarfs based on APOGEE spectra are compared to those of FGK stars from several works ([Adibekyan et al. 2012](#); [Bensby et al. 2014](#); [Chen et al. 2000](#); [Brewer & Fischer 2018](#)) in Fig. 7 of [Souto et al. \(2022\)](#). In both cases the regions covered by the M-dwarfs are consistent with those of the FGK dwarfs. There are two stars in common in the samples of [Ishikawa et al. \(2020\)](#) and [Souto et al. \(2022\)](#) for which the abundances derived from the two different observations and methods can be compared directly

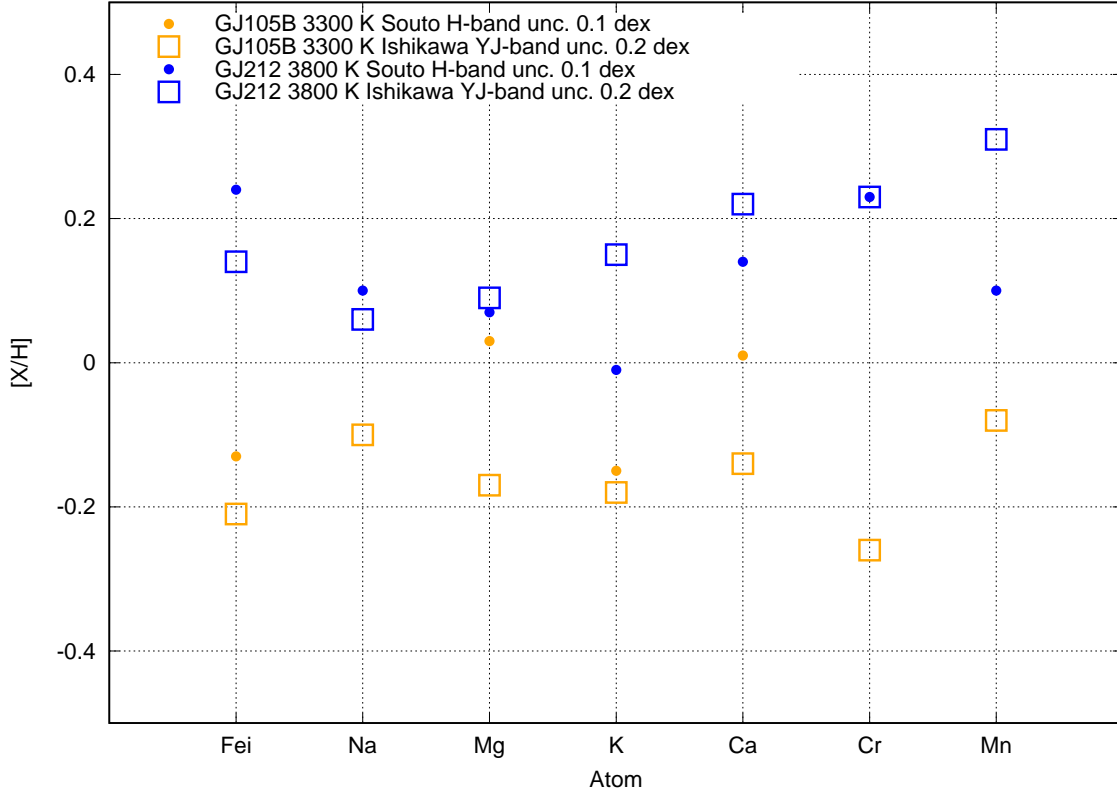


Figure 2. Comparison of element abundances from Ishikawa et al. (2020) and Souto et al. (2022) for two M dwarfs (see Sect. 3).

(the cooler slightly metal-poor star GJ 105B and the warmer slightly metal-rich star GJ 212). Fig. 2 shows that the abundances agree within the uncertainties.

In conclusion, the prospects for deriving individual element abundances for M dwarfs are promising, as the required instruments and methods have become available. The studies published so far, although somewhat limited in sample size, show consistency for abundances of binary components, for abundances from Y/J-band spectra and H-band spectra, and for abundances of M- and FGK-star samples as a whole. However, uncertainties are in general large, and ways to improve the quality of the abundances should be investigated. Furthermore, a number of caveats appear to be inherent in the abundance analysis of M dwarfs. To name a few, for the correct determination of the abundance of any element, abundances of all other elements need to be determined consistently, in particular for electron donors such as Na and Ca, which influence the continuous opacity, and for atoms which form molecules at lower T_{eff} , such as Ti and O. Other limiting factors are the (low) quality of atomic and molecular data used for the synthesis of spectral lines, non-LTE effects, for example on K lines (Olander et al. 2021), or the treatment of collisional broadening by H_2 molecules. Care has to be taken when calculating and interpolating atmospheric models for M dwarfs (see e.g. Sect. 8). Finally, the presence of magnetic fields can cause extra line broadening and intensification (these effects could be mitigated by selecting insensitive lines).

4. SPHINX II: FLAT TRANSMISSION SPECTRA FOR SMALL PLANETS WITH JWST - BUT FIRST, DO WE UNDERSTAND THE HOST STAR WELL ENOUGH?

Aishwarya R. Iyer, Michael R. Line, Jonathan J. Fortney, Philip S. Muirhead, Ehsan Gharib-Nezhad

M-dwarfs are a dominant stellar class representing a significant population of our Galaxy. Spanning a wide range of masses to the hydrogen burning limit, they endure varying physical processes in their atmospheres. Characterizing dust/cloud condensation, convection, and activity-induced photospheric effects such as spots pose tremendous challenges. Notably, [Iyer & Line \(2020\)](#) showed that with JWST spectrophotometric precisions; despite star-planet joint retrievals and corrections for the Transit Light Source Effect, transmission spectra of small planets around spotty-M-dwarfs will still yield biased inferences on the planetary atmosphere—if we do not understand the disk-integrated spectrum of the host correctly. We address this with efforts to improve M-dwarf atmosphere models.

We present SPHINX II, with a gray cloud model mimicking suppression of flux at shorter wavelengths and reddening at longer wavelengths. We improve the convection model with a reduced mixing length value increasing the depth of the convective envelope relative to the sun. We perform validation tests for SPHINX II by acquiring atmospheric properties for 32 mid-to-late-type M-dwarfs with low-resolution data taken from SpeX Prism Library and with SpeX IRTF spectra of 39 mid-to-late-type M-dwarfs that are companions to FGKM primaries observed by [Mann et al. \(2014\)](#). Our model-derived values have comparable precision as the empirical constraints of 0.078 dex in metallicities and $\sigma=0.13$ for C/O ratios.

5. ADVANCING CHEMICAL ANALYSIS OF COOL DWARFS WITH CARMENES

David Montes, Yutong Shan, Hugo M. Tabernero, et al.

The chemical connection between stars and exoplanets is key to modern planetary science. To make progress in measuring the chemical composition of cool dwarfs, we require high-resolution spectroscopic data. The CARMENES spectrograph has produced high-quality, $R \sim 90,000$ spectra in the optical and NIR for hundreds of nearby, late K and M dwarfs. The wide wavelength coverage (5600 — 17100 Å) of the CARMENES channels offers the possibility of characterising many chemical species. These spectra have been combined into a single high-quality and telluric-free spectrum per target, making them suitable for detailed abundance analysis.

Chemical elements that have already been investigated in detail using this data include Mg, Si, Rb, and V for many M dwarfs in our sample, which are relevant for understanding planetary structure and Galactic chemical evolution. We preview ongoing work using CARMENES spectra to study a number of other elements and benchmark them using wide binaries. We demonstrate that the ability to work with a large number of atomic features and stars enables better calibration of abundance measurements and characterisation of their precision for cool stars. More detailed information on CARMENES spectroscopy of M dwarfs can be found in [Abia et al. \(2020\)](#); [Marfil et al. \(2021\)](#); [Shan et al. \(2021\)](#); [Nagel et al. \(2023\)](#); [Tabernero et al. \(2024\)](#).

6. AN EXPLORATION OF OPTICAL COOL DWARF CHEMISTRY WITH BOTH DATA-DRIVEN AND PHYSICAL MODELS

Adam Rains, Thomas Nordlander, Stephanie Monty, Andrew R. Casey, Bárbara Rojas-Ayala, Maruša Žerjal, Michael J. Ireland, Luca Casagrande, and Madeleine McKenzie

Detailed chemical studies of F/G/K—or Solar-type stars—have long been routine in stellar astrophysics, enabling studies in both Galactic chemodynamics, and exoplanet demographics. However, similar understanding of the chemistry of M and late-K dwarfs—the most common stars in the Galaxy—has been greatly hampered both observationally and theoretically by the complex molecular chemistry of their atmospheres.

Here I present an extension to our recently published (Rains et al. 2024) implementation of the data-driven Cannon model (Ness et al. 2015) for cool dwarf T_{eff} , $\log g$, $[\text{Fe}/\text{H}]$, and $[\text{Ti}/\text{Fe}]$ as trained on low-to-medium resolution optical spectra (4000-7000 Å). With an updated training sample double the size of our published sample, we are able to provide more reliable parameters over a broader range of stellar T_{eff} , $[\text{Fe}/\text{H}]$, and $[\text{Ti}/\text{Fe}]$. Alongside this, we also investigated the sensitivity of optical wavelengths to various atomic and molecular species using both data-driven and theoretical means via a custom grid of MARCS synthetic spectra (Gustafsson et al. 2008), and make recommendations for where MARCS struggles to reproduce cool dwarf fluxes. Under leave-one-out cross-validation, our published Cannon model is capable of recovering T_{eff} , $\log g$, $[\text{Fe}/\text{H}]$, and $[\text{Ti}/\text{Fe}]$ with precisions of 1.4%, 0.04 dex, 0.10 dex, and 0.06 dex respectively, with the recovery of $[\text{Ti}/\text{Fe}]$ pointing to the as-yet mostly untapped potential of exploiting the abundant—but complex—chemical information within optical spectra of cool stars.

7. STARS AND THEIR PLANETS: HOW THE ANALYSIS OF HOST STAR CAN INFLUENCE OUR KNOWLEDGE OF ROCKY PLANET’S INTERIOR STRUCTURE?

Henrique Reggiani, Alejandro Ross, Kevin C. Schlaufman, Mykhaylo Plotnykov, and Diana Valencia

Exoplanet mass and radius are needed to constraint the internal structure of rocky exoplanets. However, exoplanet mass and radius directly depend on our knowledge about the host star mass and radius. Despite the importance of the host star fundamental parameters, published exoplanetary internal structure constraints have often been based on stellar inferences that are not self-consistent. We present an analysis of 24 stellar systems that host rocky exoplanets to study the dependence of exoplanet internal structure constraint on the stellar inferences. We homogeneously and self-consistently analyze the host stars using the methodology presented at Reggiani et al. (2022), and compare our results to the estimated photospheric and fundamental stellar parameters calculated using different methodologies. We compare our results with data from the APOGEE survey (Majewski et al. 2017) and from Brewer & Fischer (2016, 2018).

In Figure 3 we show that the stellar masses based on the stellar parameters calculated using our methodology, APOGEE DR 17, and from Brewer & Fischer (2016, 2018). As we can see, there are not large differences between the methodologies, and the results agree well with each other, with mean deviations in the estimated masses on the order of $\leq 0.03 M_{\odot}$. With Doppler and transit observables gathered from the literature we also recalculated the planetary masses and radii, and we show in Figure 4 that we find good agreement on the planetary masses regardless of the methodologies used to estimate stellar masses.

Our study, that will be fully presented at Ross et al. (submitted), also verified the existence of a statistically significant positive relationship between the mass radius-based core-mass fractions of terrestrial exoplanets and the metallicities of their host stars. For the first time, we show that this relationship is robust to the source of photospheric stellar parameters on which host star masses and radii and consequently terrestrial exoplanet masses and radii are based.

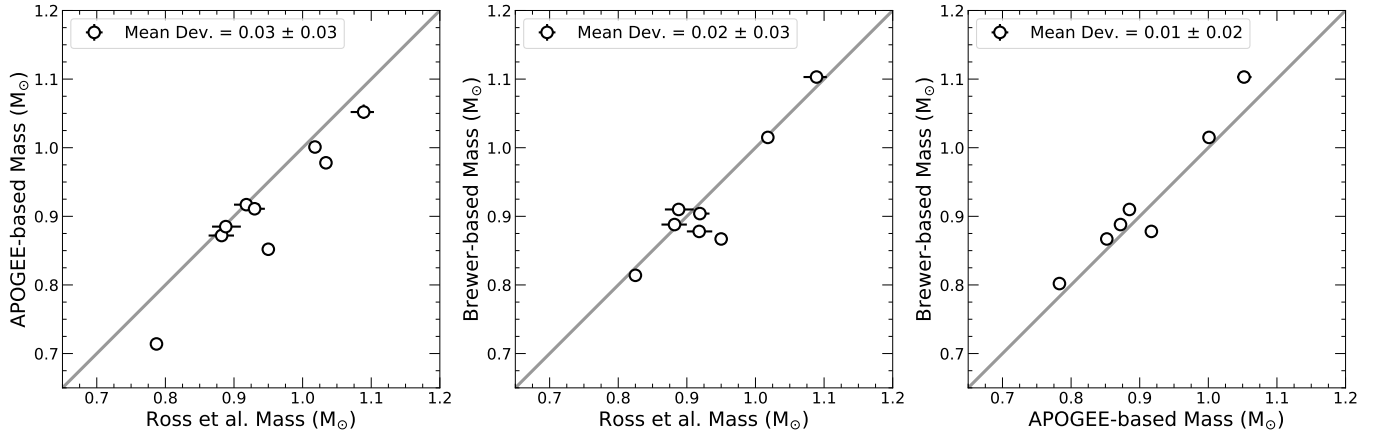


Figure 3. Comparisons of inferred stellar masses and radii based on our approach using as inputs photospheric stellar parameters from our analyses, APOGEE DR17, and [Brewer & Fischer \(2016\)](#) and [Brewer & Fischer \(2018\)](#).

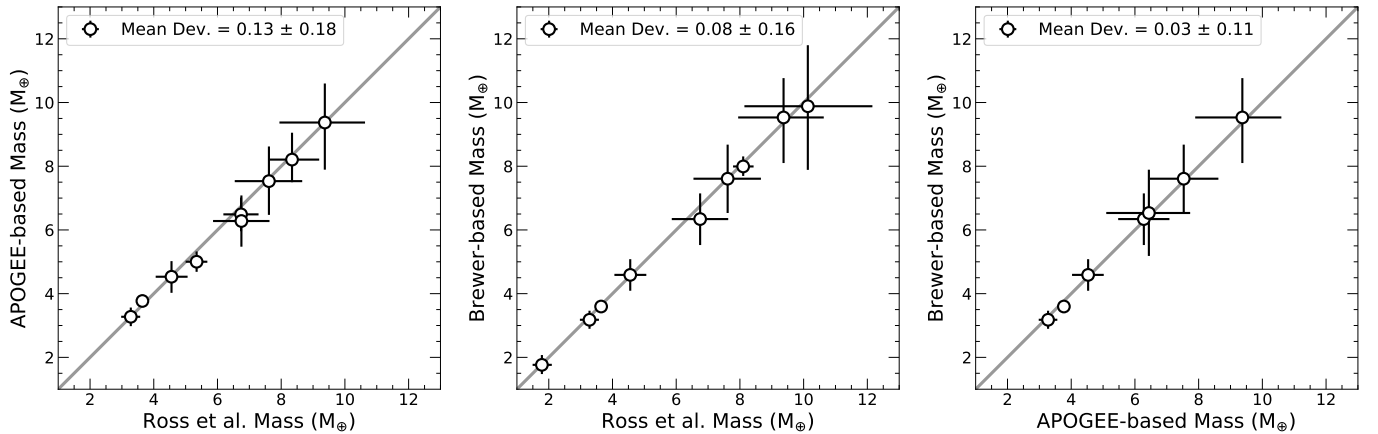


Figure 4. Comparisons of updated planetary masses from our approach using Doppler and transit observables and accurate, precise, homogeneous, and physically self consistent stellar masses and radii based on photospheric stellar parameters from our analyses, APOGEE DR17, and [Brewer & Fischer \(2016\)](#) and [Brewer & Fischer \(2018\)](#).

8. KORG, A NEW CODE FOR SPECTRAL SYNTHESIS, AND MODEL ATMOSPHERE INTERPOLATION AS A PRECISION BOTTLENECK FOR M-DWARF SPECTRA

Adam Wheeler, Andrew Casey, Matthew Abruzzo, Melissa Ness

Large spectroscopic surveys pose a computational challenge for spectroscopists because dataset of $10^5 - 10^7$ spectra cannot be analysed using traditional methods. Survey pipelines struggle to balance accuracy and resource-usage, and many systematic errors in their stellar parameters and abundances are surely introduced by the methodological compromises they are forced to make for

the sake of efficiency. As a step towards addressing this challenge, we introduce Korg, a new open-source spectral synthesis code which is compatible with automatic differentiation tools, fast enough to enable on-the-fly fitting, significantly broadening the set of possible analyses (Wheeler et al. 2023, 2024).

As discussed extensively in this session, measuring spectroscopic parameters and elemental abundances of M dwarfs can be difficult, primarily due to the presence of molecules in their atmospheres, which complicate both the equation of state and the opacity. We argue that the common practice of using model atmospheres (1D structure calculations) which are not fully consistent with the radiative transfer calculations. We demonstrate that common methods used to interpolate model atmospheres can result in flux errors at the several-percent level, and parameters often not varied in the model atmosphere (e.g. carbon abundance) have an even larger effect.

9. STELLAR PARAMETER ESTIMATION FOR M DWARFS FROM LAMOST DR10 BASED ON CYCLE-STARNET

Shuo Zhang, Hua-Wei Zhang, Yuan-Sen Ting, Rui Wang, Teaghan O’Brian, Hugh R. A. Jones

As the most common and numerous stellar members of the Milky Way galaxy and key candidates for hosting terrestrial planets, M dwarfs are of significant importance in various astronomical studies. This work provides radial velocities (RV) and three basic atmospheric parameters (T_{eff} , $\log g$, $[M/H]$) for over 500,000 M dwarfs with signal-to-noise ratio (S/N) greater than 5 in LAMOST DR10. Figure 5 shows the distribution of these M dwarfs in the equatorial coordinate system.

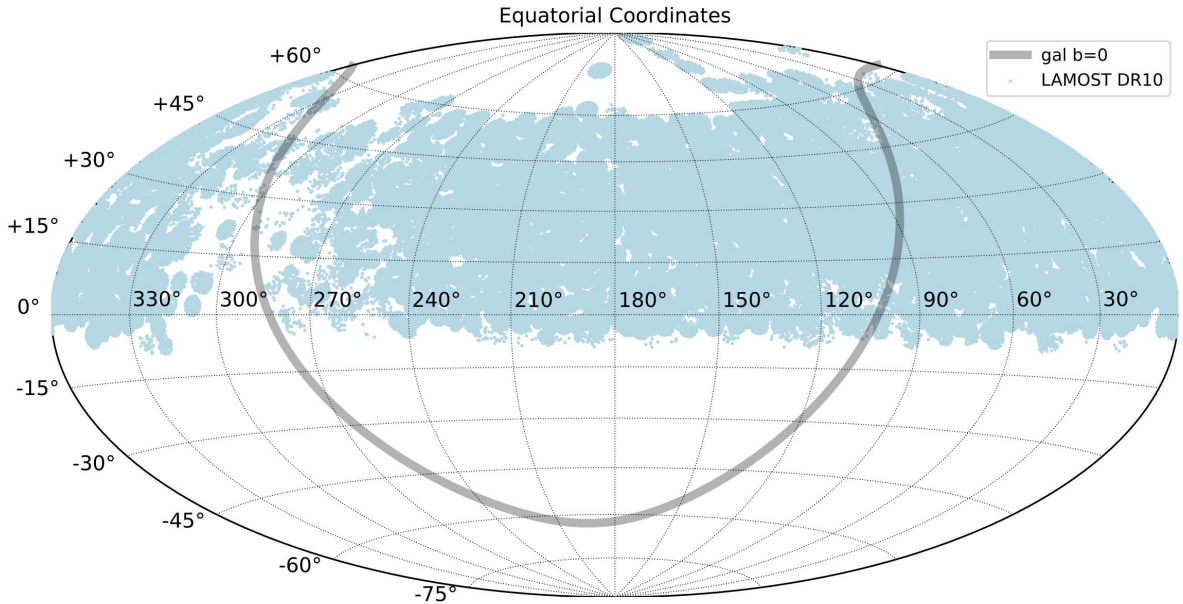


Figure 5. Distribution of the M dwarfs from LAMOST DR10 in the equatorial coordinate system.

Utilizing the domain-adaptation approach Cycle-StarNet, we bridged the gap between LAMOST low-resolution observed spectra ($R \sim 1800$) and PHOENIX synthetic spectra. The information from the PARSEC stellar evolution model constrained the parameter space of the synthetic domain, reducing errors due to parameter degeneracy. The accuracy of T_{eff} , $\log g$ and $[M/H]$ derived from comparison to available high-resolution measurements in the literature are 11 ± 71 K, 0.03 ± 0.13 dex, and 0.05 ± 0.2 dex, respectively. The Kiel diagram of the M dwarfs is shown in Figure 6. For the result of RV measurements, we achieved noise-limited precision down to 3.5 km/s. The paper is

in preparation and will be submitted soon. The complete catalog can be assessed from the url: <https://zenodo.org/records/13765284>.

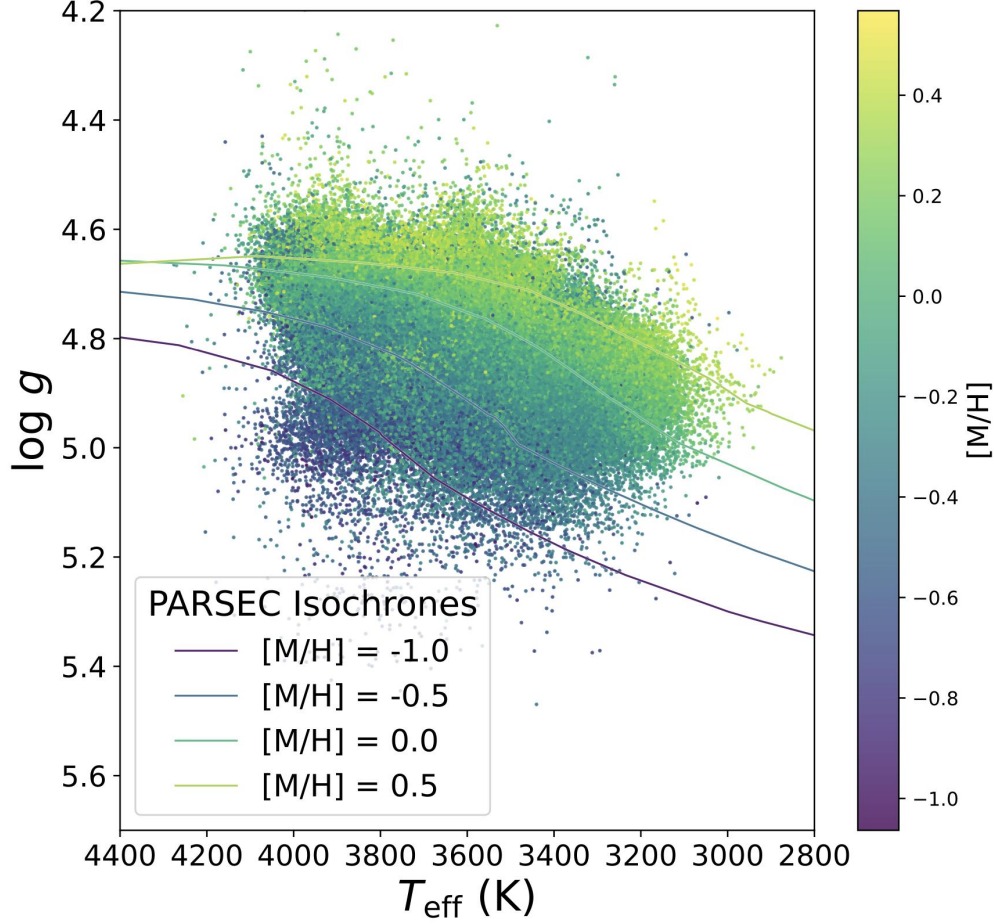


Figure 6. The distribution of over 500,000 M dwarfs from LAMOST DR10 on the Kiel diagram. The data points are color-coded according to the measured overall metallicity ($[M/H]$). Isochrones from the 5 Gyr PARSEC model are overlaid as solid lines for reference.

10. ORAL POSTER PRESENTATIONS

We list the posters that were briefly presented in the session as follows:

- A fast NLTE Radiative Transfer Emulator Based on Neural Network for Stellar Activity
Chang et al., Imperial College London, Poster# 70
- Modelling stellar transition regions of F-G stars with advanced ionisation equilibrium
Deliporanidou & Del Zanna, University of Cambridge, Poster# 30, doi:10.5281/zenodo.13209885
- Low-resolution spectral indices to derive M-dwarf abundances using wide binary systems
Duque-Arribas et al., Universidad Complutense de Madrid, Digital poster, doi:10.5281/zenodo.13220961
- M Dwarfs from the Bottom Up: SPHINX M Dwarf Structure and Evolution
Fortney et al., University of California, Santa Cruz, Digital poster

- Demographics of Giant Exoplanets from a Combination of Direct Imaging and Radial Velocity Surveys
Klusmeyer et al., New Mexico State University, Poster# 79
- Like Star like Planet: How Do Planet Properties Affect the Chemistry of Planet-Hosting Stars?
Mendez & Ezzeddine, University of Florida, Poster# 53
- The PEPSI ultra-high resolution spectral library of M dwarfs
Shan et al., Centre for Planetary Habitability, University of Oslo and Institut für Astrophysik, Georg-August-Universität, Digital poster Doi:10.5281/zenodo.13284685

The abstracts of the above-mentioned posters can be found in the website of Cool Stars 22:
https://coolstars22.github.io/docs/CS22_Abstract_booklet.pdf

Acknowledgements: We would like to extend our deepest appreciation to the scientific organizing committee and the local organizing committee of the Cool Stars 22 conference for holding the meeting.

N.H. and I.J.M.C. acknowledge support from NSF AAG grant No. 2108686 and from NASA ICAR grant No. NNH19ZDA001N. U.H. acknowledges support from the Swedish National Space Agency (SNSA/Rymdstyrelsen). E.M. acknowledges financial support through a "Margarita Salas" postdoctoral fellowship from Universidad Complutense de Madrid, funded by the Spanish Ministerio de Universidades with NextGeneration EU funds. D.M. acknowledges financial support from the Spanish Agencia Estatal de Investigación of the Ministerio de Ciencia, Innovación y Universidades (AEI/10.13039/501100011033) and the ERDF "A way of making Europe" through project PID2022-137241NB-C44. Z.Z. acknowledges support from the NASA Hubble Fellowship grant HST-HF2-51522.001-A. A.I. acknowledges support from NASA Postdoctoral Fellowship and NASA FINESST Award 80NSSC21K1846 for this work. A.D.R. acknowledges support by the Knut and Alice Wallenberg Foundation (grant 2018.0192). YP's investigations were carried out under the MSCA4Ukraine program, project number 1.4-UKR-1233448-MSCA4Ukraine, which is funded by the European Commission. V.A. is supported by Fundação para a Ciência e Tecnologia through national funds and by FEDER through COMPETE2020 - Programa Operacional Competitividade e Internacionalização by these grants: UIDB/04434/2020; UIDP/04434/2020; 2022.06962.PTDC.

REFERENCES

- | | |
|--|---|
| <p>Abia, C., Tabernero, H. M., Korotin, S. A., et al. 2020, A&A, 642, A227. doi:10.1051/0004-6361/202039032</p> <p>Adibekyan, V. Z., Sousa, S. G., Santos, N. C., et al. 2012, A&A, 545, A32. doi:10.1051/0004-6361/201219401</p> <p>Barrado, D., Mollière, P., Patapis, P., et al. 2023, Nature, 624, 263. doi:10.1038/s41586-023-06813-y</p> <p>Adibekyan, V., Dorn, C., Sousa, S. G., et al. 2021, Science, 374, 330. doi:10.1126/science.abg8794</p> <p>Bedell, M., Bean, J. L., Meléndez, J., et al. 2018, ApJ, 865, 68. doi:10.3847/1538-4357/aad908</p> <p>Bensby, T., Feltzing, S., & Oey, M. S. 2014, A&A, 562, A71. doi:10.1051/0004-6361/201322631</p> <p>Bergin, E. A., Bosman, A., Teague, R., et al. 2024, ApJ, 965, 147. doi:10.3847/1538-4357/ad3443</p> | <p>Bond, J. C., O'Brien, D. P., & Lauretta, D. S. 2010, ApJ, 715, 1050. doi:10.1088/0004-637X/715/2/1050</p> <p>Botelho, R. B., Milone, A. de C., Meléndez, J. 2020, MNRAS, 499, 2196. doi:10.1093/mnras/staa2917</p> <p>Brewer, J. M., & Fischer, D. A. 2016, ApJ, 831, 20. doi:10.3847/0004-637X/831/1/20</p> <p>Brewer, J. M. & Fischer, D. A. 2018, ApJS, 237, 38. doi:10.3847/1538-4365/aad501</p> <p>Brugger, B., Mousis, O., Deleuil, M., & Deschamps, F. 2017, ApJ, 850, 93. doi:10.3847/1538-4357/aa965a</p> <p>Chen, Y. Q., Nissen, P. E., Zhao, G., et al. 2000, A&AS, 141, 491. doi:10.1051/aas:2000124</p> <p>Coria, D. R., Crossfield, I. J. M., Lothringer, J. 2023, ApJ, 954, 121. doi:10.3847/1538-4357/acea5f</p> |
|--|---|

- Coria, D. R., Hejazi, N., Crossfield, I. J. M., & Rhem, M. 2024, arXiv.2409.02286. doi:10.48550/arXiv.2409.02286
- Crossfield, I. J. M., Lothringer, J. D., Flores, B., et al. 2019, *ApJL*, 871, L3. doi:10.3847/2041-8213/aaf9b6
- Crossfield, I. J. M. 2023, *ApJL*, 952, L18. doi:10.3847/2041-8213/ace35f
- Delgado Mena, E., Adibekyan, V., Santos, N. C., et al. 2021, *A&A*, 655, A99. doi:10.1051/0004-6361/202141588
- Dorn, C., Khan, A., Heng, K., et al. 2015, *A&A*, 577, A83. doi:10.1051/0004-6361/201424915
- Dorn, C., Venturini, J., Khan, A., et al. 2017, *A&A*, 597, A37. doi:10.1051/0004-6361/201628708
- Dressing, C. D., & Charbonneau, D. 2013, *ApJ*, 767, 95. doi:10.1088/0004-637X/767/1/95
- Dressing, C. D., & Charbonneau, D. 2015, *ApJ*, 807, 45. doi:10.1088/0004-637X/807/1/45
- Gustafsson B., Edvardsson B., Eriksson K., Jørgensen U. G., Nordlund Å., Plez B., 2008, *A&A*, 486, 951. doi:10.1051/0004-6361:200809724
- Hardegree-Ullman, K. K., Cushing, M. C., Muirhead, P. S., & Christiansen, J. L. 2019, *AJ*, 158, 75. doi:10.3847/1538-3881/ab21d2
- Hinkel, N. R., & Unterborn, C. T. 2018, *ApJ*, 853, 83. doi:10.3847/1538-4357/aaa5b4
- Fortney, J. J. 2012, *ApJL*, 747, L27. doi:10.1088/2041-8205/747/2/L27
- Hejazi, N., Lepine, S., & Nordlander, T. 2022, 927, 122. doi:10.3847/1538-4357/ac4e16
- Hejazi, N., Crossfield, I. J. M., Nordlander, T., et al. 2023, *ApJ*, 949, 79. doi:10.3847/1538-4357/accb97
- Hejazi, N., Crossfield, I. J. M., Souto, D., et al. 2024, *ApJ*, 973, 31. doi:10.3847/1538-4357/ad61dc
- Ishikawa, H. T., Aoki, W., Kotani, T., et al. 2020, *PASJ*, 72, 102. doi:10.1093/pasj/psaa101
- Ishikawa, H. T., Aoki, W., Hirano, T., et al. 2022, *AJ*, 163, 72. doi:10.3847/1538-3881/ac3ee0
- Iyer, A. R. & Line, M. R. 2020, *ApJ*, 889, 78. doi:10.3847/1538-4357/ab612e
- Lindgren, S., Heiter, U., & Seifahrt, A. 2016, *A&A*, 586, A100. doi:10.1051/0004-6361/201526602
- Lindgren, S., & Heiter, U. 2017, *A&A*, 604, A97. doi:10.1051/0004-6361/201730715
- López-Valdivia, R., Mace, G. N., Sokal, K. R. 2019, *ApJ*, 879, 105. doi:10.3847/1538-4357/ab2129
- Luo, H., Dorn, C., & Deng, J. 2024, arXiv:2401.16394. doi:10.48550/arXiv.2401.16394
- Majewski, S. R., Schiavon, R. P., Frinchaboy, P. M., et al. 2017, *AJ*, 154, 94. doi:10.3847/1538-3881/aa784d
- Maldonado, J., Micela, G., Baratella, M., et al. 2020, *A&A*, 644, A68. doi:10.1051/0004-6361/202039478
- Mann, A. W., Deacon, N. R., Gaidos, E., et al. 2014, *AJ*, 147, 160. doi:10.1088/0004-6256/147/6/160
- Marfil, E., Tabernero, H. M., Montes, D., et al. 2021, *A&A*, 656, A162. doi:10.1051/0004-6361/202141980
- Melo, E., Souto, D., Cunha, K., et al. 2024, arXiv.2406.00111. doi:10.48550/arXiv.2406.00111
- Nagel, E., Czesla, S., Kaminski, A., et al. 2023, *A&A*, 680, A73. doi:10.1051/0004-6361/202346524
- Ness M., Hogg D. W., Rix H.-W., Ho A. Y. Q., Zasowski G., 2015, *ApJ*, 808, 16. doi:10.1088/0004-637X/808/1/16
- Nomura, H., Furuya, K., Cordiner, M. A., et al. 2023, *Protostars and Planets VII*, *Astronomical Society of the Pacific Conference Series*, 534, 1075
- Öberg, K. I., Murray-Clay, R., & Bergin, E. A. 2011, *ApJ*, 758, 36. doi:10.1088/0004-637X/758/1/36
- Olander, T., Heiter, U., & Kochukhov, O. 2021, *A&A*, 649, A103. doi:10.1051/0004-6361/202039747
- Passegger, V. M., Reiners, A., Jeffers, S. V., et al. 2018, *A&A*, 615, A6. doi:10.1051/0004-6361/201732312
- Passegger, V. M., Schweitzer, A., Shulyak, D., et al. 2019, *A&A*, 627, A161. doi:10.1051/0004-6361/201935679
- Passegger, V. M., Bello-García, A., Ordieres-Meré, J., et al. 2022, *A&A*, 658, A194. doi:10.1051/0004-6361/202141920
- Pavlenko Y., Tennyson, J., Yurchenko, S. N. et al. 2022, *MNRAS*, 516, 5655. doi: 10.1093/mnras/stac2588.
- Pavlenko, Ya. V., Yurchenko, S. N., McKemmish, L. K. et al. 2021, *A&A*, 642, A77. doi: 10.1051/0004-6361/202037863
- Rains A. D., Nordlander T., Monty S., Casey A. R., Rojas-Ayala B., Žerjal M., Ireland M. J., et al., 2024, *MNRAS*, 529, 3171. doi:10.1093/mnras/stae560
- Rajpurohit, A. S., Reylé, C., Allard, F., et al. 2014, *A&A*, 564, A90. doi:10.1051/0004-6361/201322881
- Rajpurohit, A. S., Allard, F., Rajpurohit, S., et al. 2018, *A&A*, 620, A180. doi:10.1051/0004-6361/201833500
- Reggiani, H., Schlaufman, K. C., Healy, B. F., et al. 2022, *AJ*, 163, 159. doi:10.3847/1538-3881/ac4d9f
- Rogers, L. A., & Seager, S. 2010, *ApJ*, 712, 974. doi:10.1088/0004-637X/712/2/974
- Santos, N. C., Adibekyan, V., Mordasini, C., et al. 2015, *A&A*, 580, L13. doi:10.1051/0004-6361/201526850
- Seager, S., Kuchner, M., Hier-Majumder, C. A., & Militzer, B. 2007, *ApJ*, 669, 1279. doi:10.1086/521346
- Shan, Y., Reiners, A., and Fabbian, D., et al. 2021, *A&A*, 654, A118. doi:10.1051/0004-6361/202141530
- Souto, D., Cunha, K., García-Hernández, D. A., et al. 2017, *ApJ*, 835, 239. doi:10.3847/1538-4357/835/2/239
- Souto, D., Cunha, K., Smith, V. V., et al. 2020, *ApJ*, 890, 133. doi:10.3847/1538-4357/ab6d07

- Souto, D., Cunha, K., & Smith, V. V. 2021, *ApJ*, 917, 11, doi:10.3847/1538-4357/abfdb5
- Souto, D., Cunha, K., Smith, V. V., et al. 2022, *ApJ*, 927, 123. doi:10.3847/1538-4357/ac4891
- Tabernero, H. M., Shan, Y., Caballero, J. A., et al. 2024, *A&A*, 689, A223. doi:10.1051/0004-6361/202450054
- Thiabaud, A., Marboeuf, U., Alibert, Y., Leya, I., & Mezger, K. 2015, *A&A*, 580, A30. doi:10.1051/0004-6361/201525963
- Tsuji, T. 2016, *Publications of the Astronomical Society of Japan*, 68, 84. doi:10.1093/pasj/psw076
- Tuomi, M., Jones, R. A., Barnes, J. R., et al. 2014, *MNRAS*, 441, 1545. doi:10.1093/mnras/stu358
- Turrini, D., Schisano, E., Fonte, S., et al. 2021, *ApJ*, 909, 40. doi:10.3847/1538-4357/abd6e5
- Unterborn, C. T., Desch, S. J., Hinkel, N. R., & Lorenzo, A. 2018, *Nature Astronomy*, 2, 297. doi:10.1038/s41550-018-0411-6
- Unterborn, C. T., Desch, S. J., Haldemann, J., et al. 2023, *ApJ*, 944, 42. doi:10.3847/1538-4357/acia3b
- Valencia, D., Sasselov, D. D., & O’Connell, R. J. 2007, *ApJ*, 656, 545. doi:10.1086/509800
- Veyette, M. J., Muirhead, P. S., Mann, A. W., et al. 2017, *ApJ*, 851, 26. doi:10.3847/1538-4357/aa96aa
- Wanderley, F., Cunha, K., Souto, D., et al. 2023, *ApJ*, 951, 90. doi:10.3847/1538-4357/acd4bd
- Wheeler, A. J., Abruzzo, M. W., Casey, A. R., & Ness, M. K. 2023, *AJ*, 165, 68. doi:10.3847/1538-3881/aciaad
- Wheeler, A. J., Casey, A. R., & Abruzzo, M. W. 2024, *AJ*, 167, 83. doi:10.3847/1538-3881/ad19cc
- Xuan, J. W., Wang, J., Finnerty, L., et al. 2024, *ApJ*, 962, 10. doi:10.3847/1538-4357/ad1243
- Yoshida, T. C., Nomura, H., Furuya, K., et al. 2024, *ApJ*, 966, 63. doi:10.3847/1538-4357/ad2fb4
- Zhang, K., Bergin, E. A., Blake, G. A., et al. 2017, *Nature Astronomy*, 1, 0130. doi:10.1038/s41550-017-0130
- Zhang, S., Luo, A. L., Comte, G., et al. 2021, *ApJ*, 908, 131. doi:10.3847/1538-4357/abcf5
- Zhang, Y., Snellen, I. A. G., Bohn, A. J., et al. 2021a, *Nature*, 595, 370. doi:10.1038/s41586-021-03616-x
- Zhang, Y., Snellen, I. A. G., & Mollière, P. 2021b, *A&A*, 656, A76. doi:10.1051/0004-6361/202141502